

## INTRODUCTION

Chronic liver disease is a major public health problem worldwide. Liver fibrosis, a common feature of almost all causes of chronic liver disease, involves the accumulation of collagen, proteoglycans, and other macromolecules within the extracellular matrix. Fibrosis tends to progress, leading to hepatic dysfunction, portal hypertension, and ultimately cirrhosis (*Faria et al., 2009*).

Accurate staging of liver fibrosis -commonly determined by liver biopsy- is critical because it determines the indication of antiviral treatment and prognosis of patients with chronic viral hepatitis (*Do et al., 2010*). However, liver biopsy is relatively invasive, limited by sample size, and difficult to repeat. Thus, noninvasive tools to assess the degree of fibrosis of the whole liver are urgently needed. Several noninvasive MRI techniques have been investigated for the diagnosis of liver fibrosis and cirrhosis, including diffusion-weighted imaging, MR elastography, and perfusion-weighted imaging. Diffusion-weighted imaging is a particularly appealing method for the diagnosis of liver fibrosis because it is easy to implement and process, without the need for contrast agents (*Do et al., 2010*).

Hepatocellular carcinoma is the most common primary malignancy of the liver, with an annual incidence of more than

1 million worldwide. (*Kalva et al., 2008*). The liver is also a common site of metastatic disease. For instance, more than 14,5000 cases of colorectal cancer are diagnosed each year, and hepatic metastases develop in approximately half of those cases. The liver is a frequent site of metastases from colorectal cancer because of portal venous drainage of the bowel. In most patients, metastases from colorectal cancer affect only the liver. (*Kalva et al., 2008*).

Egypt has the highest prevalence of hepatitis C virus (HCV) all over the world, with an estimated 8-10 million among a population of 68 million having been exposed to the virus and 5-7 million active infections. It is considered the most common aetiology of chronic liver disease (CLD) in Egypt, where prevalence of antibodies to HCV (anti-HCV) is 10-fold greater than the United States and Europe (*Goldstone et al., 2002; Strickland et al., 2002*).

Accurate detection and characterization of focal hepatic lesions is important for treatment planning in patients with hepatic tumors. For the detection and characterisation of hepatic lesions, CT and MRI are usually employed (*Yang et al., 2011*). MRI, T1 weighted, T2 weighted and gadolinium-enhanced T1 weighted imaging have been commonly utilized (*Yang et al., 2011*).

As a result of recent advances in MR technology, DWI is now feasible outside the brain with improved image quality and

promising results. This noncontrast technique is easy to implement in clinical practice as it can be added to existing protocols without significant time penalty. Diffusion-weighted imaging quantifies thermally induced motion of water molecules known as Brownian motion in tissue (*Chandrana et al., 2010*).

Highly cellular tissues, such as tumors, will show restricted diffusion (high signal intensity) on the higher b-values (greater than or equal 400-500 s/mm<sup>2</sup>) images and correspondingly lower ADC values, whereas less cellular benign lesions tend to have a relatively lower signal intensity on the high b-value images with corresponding high ADC values (*Chandrana et al., 2010*).

Using DWI, simple and ciliated hepatic foregut cysts and liver cysts in polycystic kidney disease show a signal intensity decrease with increasing b-values, and are strongly hyperintense and homogeneous on analog-to-digital (ADC) sequences (*Ba-Ssalamah et al., 2010*).

On DWI, hemangiomas show signal intensity loss with increased b-values and typically show high signal intensity on ADC map. However, a confident differentiation between cystic metastases and hemangioma cannot be achieved solely with this single pulse sequence and should be interpreted in conjunction with contrast-enhanced images (*Ba-Ssalamah et al., 2010*).

As a solid tumor, an adenoma shows slight signal intensity increase with increasing b-values on DWI and appears hypointense on ADC maps. The ADC value ranges between 1 and  $1.4 \times 10^{-3} \text{ mm}^2/\text{s}$  cm/s. However, the ADC values may overlap with FNH, HCC, and other malignant solid lesions (*Ba-Ssalamah et al., 2010*).

As a solid tumor, FNH shows slightly high signal intensity with increasing b-values on DWI, and is again hypointense on ADC, with a reported ADC value between 1 and  $1.40 \times 10^{-3} \text{ mm}^2/\text{s}$  cm/s. However, the ADC values may overlap with those of other solid lesions, including adenoma and malignant lesions, and therefore cannot be relied on for lesion characterization (*Ba-Ssalamah et al., 2010*).

The main reason that DWI is able to show HCCs as hyperintense is the high cellularity of malignant tumors. In addition DWI could suppress the signals of other structures such as vascular structures and bile duct. But iso-SI or hypo-SI for DNs on DWI may be mainly due to no definite restriction of diffusion of water molecules (*Xu et al., 2010*).

The histopathologic grade of a malignant neoplasm is determined by both its cellular and structural atypia. The cellularity that DWI is believed to reflect is mainly due to structural atypia. When the DWI findings were compared with histopathologic specimens, the difference in cellularity between

DNs and HCCs was enough to be reflected by the ADC. On the contrary, the difference in cellularity among well-, moderately, and poorly differentiated HCCs was thought to be too slight to represent differences in ADC. Cellular atypia, represented mainly by nucleus-cytoplasm ratio, is not fully reflected on the current DWI sequence because it mainly describes the brownian motion of the extracellular, rather than the intracellular, water molecules (*Xu et al., 2010*).

ADC values are lower in patients with chronic liver disease and diffusion restriction caused by proteoglycan and glycosaminoglycan deposits might explain this phenomenon (*Soylu et al., 2009*).

## **AIM OF THE WORK**

**T**he aim of this work is to highlight the role of Diffusion-weighted MRI in the diagnosis of parenchymatous liver disease, and parenchymal hepatic focal lesions.

## ANATOMY OF THE LIVER

### Gross anatomy of the liver:

At the start of the fourth week of intrauterine life, the liver is one of the first organs to develop, undergoing rapid growth to fill the abdominal cavity and amounting to 10% of the total fetal weight by the ninth week of development (*Lindor and Vargas, 2011*).

The liver, biliary system, and gall bladder are said to arise as a ventral outgrowth from the caudal part of the foregut. This ventral outgrowth is described as being “ Y ” shaped and known as the hepatic diverticulum. At the same time, a thick mass of splanchnic mesoderm, the septum transversum, develops on the cranial aspect of the coelomic cavity (between the developing heart and midgut). The cranial part of the septum transversum gives rise to the pericardial cavity (and, eventually, pericardium) and the diaphragm. The caudal part is, however, soon invaded by the developing liver and, as the liver grows, it is said to become surrounded by the septum transversum, which is then referred to as the ventral mesogastrium (*Lindor and Vargas, 2011*).

As the liver grows into the ventral mesogastrium, it divides into two parts. The larger, more cranial part is the primordium of the liver. The smaller, more caudal part gives rise to the gall bladder. The stalk of the hepatic diverticulum goes on to form the cystic duct and the stalk connecting the

hepatic and cystic ducts to the duodenum forms the bile duct. It is important to note that, initially, the bile duct is attached to the ventral aspect of the duodenal loop. However, rotation of the duodenum carries the bile duct to its dorsal aspect, where it maintains its position throughout adult life (*Lindor and Vargas, 2011*).

The liver is one of the largest organs in the body, occupying at least 2-3% of the total adult body weight. It weighs roughly 1200-1500 g in the average adult (*Chouker et al., 2004*).

The liver appears wedge shaped, with its base to the right and its apex projecting to the left as it extends between the right and left upper quadrants. In its subdiaphragmatic position, the liver lies beneath the overlying ribs and cartilage. Its superior convex surface fills the concavity of the right dome of the diaphragm, reaching the fifth rib on the right and the fifth intercostals space, 7-8 cm from the midline, on the left. The upper margin may be traced at the level of the xiphisternal joint as it arches upward on each side. The right lateral margin therefore lies against the diaphragm and anterolateral thoracic wall, crossing the seventh to eleventh ribs along the midaxillary line. In comparison, the inferior border is sharp and may be followed just below the costal margin on the right extending to the left toward the fifth intercostals space. It is formed by a line joining the right lower, and upper left extremities (*Sinnatamby, 2006*).



## **Surfaces and their relations:**

*The liver has two surfaces:*

### **1. Diaphragmatic surface**

It is related to the diaphragm and has four parts which are smoothly continuous with each other.

### **2. Visceral surface or inferior surface**

It is the only surface not related to the diaphragm *fig (1.1)*. It sits upon the upper abdominal viscera which form the "liver bed" (*Halim, 2008*).

The visceral surface of the liver lies in contact with, and is slightly moulded by:

- The oesophagus, stomach and lesser omentum on the left;
- The pancreas (through the lesser omentum) and the duodenum in the midline; and
- The right kidney and adrenal and the hepatic flexure of the colon on the right (*Ryan et al., 2004*).

## **Classical anatomy**

The liver is divided into anatomical right and left lobes by the following ligaments and fissures:

- Falciform ligament, which attaches the anterior and superior surfaces of the liver to the diaphragm and the anterior abdominal wall.

- Ligamentum teres, runs forward across the inferior surface and border of the liver in a fissure to the left end of the porta hepatis, from the liver the ligamentum teres runs downward to reach the umbilicus.
- Ligamentum venosum, runs upward across the posterior surface of the liver, in a deep fissure, first forwards and then to the right. It diverges from the left end of porta hepatis (*Halim, 2008*).

The surgical subdivision into right and left lobes is defined by the following landmarks:

- Fossa for the gall bladder.
- Groove for inferior vena cava.

The fissures for the ligamentum teres and venosum, the fossa for the gall bladder, the groove for the inferior vena cava along with the porta hepatis form an H- shaped pattern on the posteroinferior aspect of the liver. The portion of liver behind the porta hepatis and between the sulcus for the inferior vena cava and fissure for ligamentum venosum is the caudate lobe, so called because it is attached to the right lobe by the tail-like caudate process. The rectangular portion of the liver between the fossa for gall bladder and the fissure for ligamentum venosum is the quadrate lobe (*Halim, 2008*).

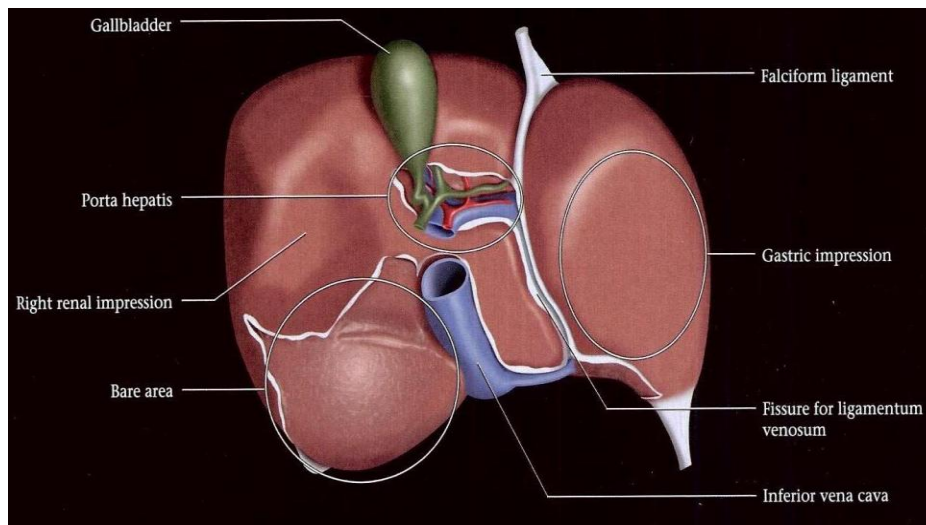


**Figure (1.1):** Hepatic visceral surface (*Federle et al., 2006*).

### **Segmental anatomy of the liver:**

Segmental anatomy is crucial in order to precisely localize a focal lesion, to evaluate a possibility of a resection, and to choose the adequate technique for resection, and finally to estimate the easiness or the difficulties of a biopsy or of any other percutaneous maneuver. Segmental anatomy is the basis of modern hepatic surgery. Each segment in fact, is supplied by a sheath containing branches of the hepatic artery and portal vein and a draining bile duct, which enters the middle of the segment. The venous drainage is by the hepatic vein, which tends to run between segmental divisions (*Vogl et al., 2003*).

## 1. Couinaud classification

The Couinaud classification of liver anatomy divides the liver into eight functionally independent segments. Each segment has its own vascular inflow, outflow and biliary drainage. In the centre of each segment there is a branch of the portal vein, hepatic artery and bile duct. In the periphery of each segment there is vascular outflow through the hepatic veins.

- Right hepatic vein divides the right lobe into anterior and posterior segments.
- Middle hepatic vein divides the liver into right and left lobes (or right and left hemiliver). This plane runs from the inferior vena cava to the gallbladder fossa.
- Left hepatic vein divides the left lobe into a medial and lateral part.
- Portal vein divides the liver into upper and lower segments. The left and right portal veins branch superiorly and inferiorly to project into the center of each segment.

### *Segments numbering fig. (1.2):*

There are eight liver segments. Segment 4 is sometimes divided into segment 4a and 4b according to Bismuth. The numbering of the segments is in a clockwise manner. Segment 1 (caudate lobe) is located posterior. It is not visible on a frontal

view. On a normal frontal view the segments 6 and 7 are not visible because they are located more posteriorly. The right border of the liver is formed by segment 5 and 8. Although segment 4 is part of the left hemiliver, it is situated more to the right. The left hepatic vein separates the medial part (segment 4) from the lateral part (segments 2 and 3). The left hepatic vein is located slightly to the left of the falciform ligament (*Smithuis, 2006*).

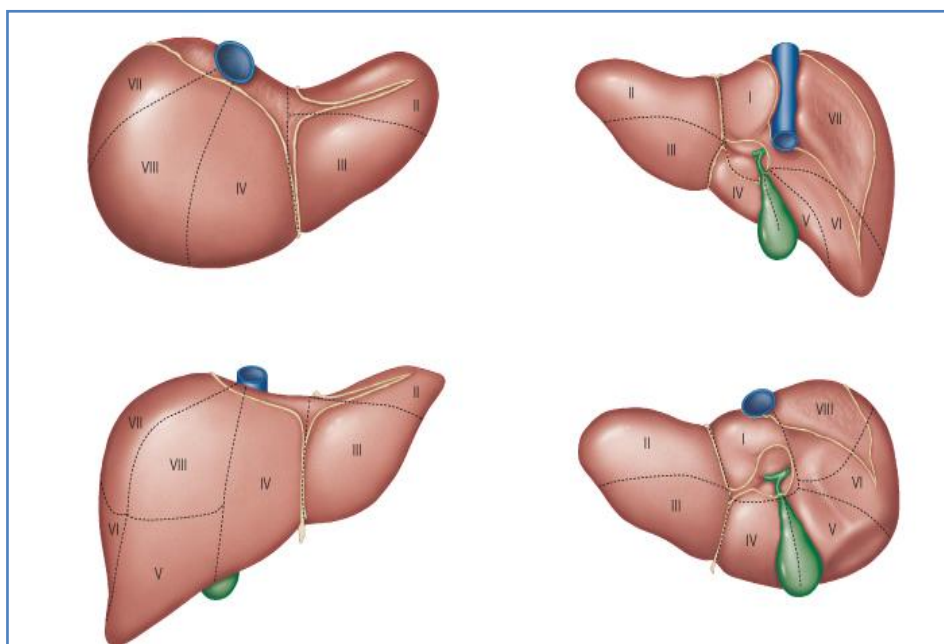


**Figure (1.2):** Showing Segmentation of the liver-  
Couinaud. (*Standring et al., 2008*).

Top left, superior view; top right, posterior view; bottom left, anterior view; bottom right, inferior view. The segments are sometimes referred to by name - I, caudate (sometimes subdivided into left and right parts); II, lateral superior; III, lateral inferior; IV, medial (sometimes subdivided into superior and inferior parts); V,

anterior inferior; VI, posterior inferior; VII, posterior superior; VIII, anterior superior.

## **2. Bismuth's classification**

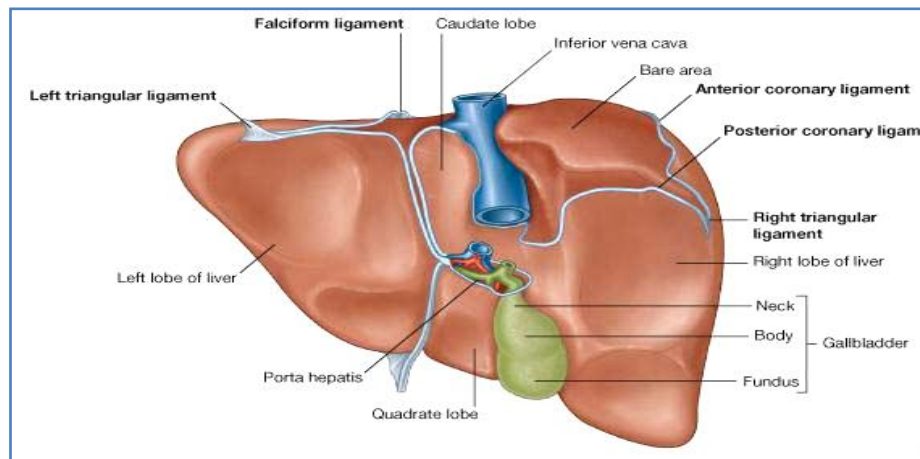
This classification is very similar to the Couinaud classification, although there are small differences. According to Bismuth three hepatic veins divide the liver into four sectors, further divided into segments. These sectors are termed portal sectors as each is supplied by a portal pedicle in the centre. The separation line between sectors contain a hepatic vein. The hepatic veins and portal pedicels are intertwined, as are the fingers of two hands. The left portal scissura divides the left liver into two sectors: anterior and posterior. Left anterior sector consists of two segments: segment IV, which is the quadrate lobe and segment III, which is anterior part of anatomical left lobe.

These two segments are separated by the left hepatic fissure or umbilical fissure. Left posterior sector consists of only one segment II. It is the posterior part of left Lobe (*Smithuis, 2006*).

### **The peritoneal connections fig. (1.3):**

The liver has a large bare surface, devoid of a peritoneal connection covering on its posterior surface. The rest of the organ is covered and is joined by peritoneal investments to neighboring structures namely the diaphragm, the stomach, duodenum, and the anterior abdominal wall. They are the right and left triangular

ligaments, the falciform ligament, the coronary ligament, and the lesser omentum (*Goldin and Banerjee, 2009*).



**Figure(1.3):** Ligaments of the liver (*Standring et al., 2008*).

### **Porta Hepatis:**

The porta hepatis is a transverse fissure separating the quadrate lobe from the caudate lobe. Its lips give attachment to the lesser omentum. The right and left branches of the hepatic artery and the portal vein enter it, and the right and left hepatic ducts come out of it. Hepatic lymph nodes and a pad of fat are situated near it. (*Halim, 2008*).

### **Blood Supply:**

The liver receives about 70% of its blood via the portal vein and 30% from the hepatic artery.

The hepatic artery commonly arises from the celiac trunk but may sometimes come off the superior mesenteric artery or